

Extreme precipitation intensity in future climates associated with the Clausius-Clapeyron-like relationship

Tomohito J. Yamada¹, Murad. A. Farukh^{1*}, Taiki Fukushima^{2**}, Masaru Inatsu³, Tomonori Sato⁴, Yadu N. Pokhrel⁵ and Taikan Oki⁶

¹Faculty of Engineering, Hokkaido University, Japan

²Graduate School of Engineering, Hokkaido University, Japan

³Faculty of Science, Hokkaido University, Japan

⁴Faculty of Environmental Earth Science, Hokkaido University, Japan

⁵Department of Civil and Environmental Engineering, Michigan State University, USA

⁶Institute of Industrial Science, The University of Tokyo, Japan

Abstract:

This paper introduces a method named “hybrid-downscaling” to estimate the future extreme hourly precipitation intensity based on observational evidence of the 99th percentile precipitation intensity against air temperature in Sapporo and Tokyo, Japan. The future projected air temperature under the Special Report on Emissions Scenarios (SRES) A1B was used after dynamical downscaling using 3 different regional atmospheric models (RAMs) with lateral boundary conditions from 3 different general circulation models (GCMs). We analyzed the 99th percentile of hourly precipitation intensity against daily mean air temperature in Sapporo and Tokyo. The 99th percentile precipitation intensity tended to have an approximate equation in which the rate of increment was similar to the Clausius-Clapeyron rate of change in the saturated water vapor. This study also showed that the precipitable water vapor and the convective instability followed the Clausius-Clapeyron-like rate of change during the hours with the 99th percentile precipitation intensity.

KEYWORDS extreme precipitation; downscaling; Clausius-Clapeyron; RAM; GCM

INTRODUCTION

The northern island of Japan, Hokkaido, is categorized as Dfa or Dfb in the Köppen-Geiger climate classification (Peel *et al.*, 2007). Sapporo has a humid continental climate and is the largest city in northern Japan with a population of approximately 2 million. The number of line-shaped rainbands with torrential precipitation has increased in the Sapporo area (Yamada *et al.*, 2012). On 23–24 August 2010, a line-shaped rainband caused 42 mm h⁻¹ of rainfall in this area setting a 53-year record. On September 10 and 11, 2014, another torrential rain event which was also associated with line-shaped rainbands caused landslides, mudslides, and flooding across Hokkaido resulting in an evacuation order for nearly 700,000 residents of 330,000 households.

According to the Japan Meteorological Agency (JMA), at least 100 mm h⁻¹ precipitation occurred overnight within around 60 km of Sapporo city in that case (EDIS, 2015). This evidence indicates that the frequency of extreme rainfall events is increasing in this region, which has been explained by Farukh and Yamada (2014) using a multivariate statistical approach. As the hydrological cycle intensifies under the projected future climate, it is likely that the frequency of such extreme hydroclimatic events will further increase. Therefore, projecting future extreme precipitation intensity has become one of the major concerns regarding climate change adaptation to prevent floods and landslides in this area.

Dynamical downscaling techniques have been widely used to estimate extreme short-term precipitation in regional atmospheric models (RAMs) by applying lateral boundary conditions obtained from general circulation models (GCMs) with different future scenarios. However, the extreme short-term precipitation intensity strongly depends on the GCM's behavior itself. Moreover, the near-surface air temperature has smaller uncertainties among GCMs compared to the precipitation (Kharin *et al.*, 2007; IPCC, 2014).

Analyzing *in situ* data some recent studies have shown the relationship between the extreme short-term precipitation intensity (such as 99th percentile; hereafter P_{99}) and the near-surface air temperature follows the Clausius-Clapeyron (CC) rate of change in saturation vapor pressure (e.g., Allen and William, 2002; Pall *et al.*, 2007; Kharin *et al.*, 2007; Muller *et al.*, 2011; Utsumi *et al.*, 2011). The CC scaling on a sub-hourly time scale was potentially applicable, even in regions where the CC scaling on a daily time scale was not applicable. Fujibe (2013) investigated the long-term changes in extreme precipitation on 10-min and hourly scales between 1951 and 2010 in Japan. Extreme 10-min and hourly precipitation, calculated from 5-year averages of annual maximum and 95th percentile values, had high correlations with temperature with a rate of $9.7 \pm 4.1\%$ and $8.8 \pm 8.3\% \text{ K}^{-1}$, respectively. These values are similar to the CC rate of change in saturated water vapor ($\sim 6\%$ per degree).

The purpose of this study is to introduce a methodology to estimate the future $P_{99}(T)$ based on observational evidence

Correspondence to: Tomohito J. Yamada, Faculty of Engineering, Hokkaido University, N13-W8, Kita-ku, Sapporo, Hokkaido 060-8628, Japan. E-mail: tomohito@eng.hokudai.ac.jp

* Present address: Department of Environmental Science, Bangladesh Agricultural University, Bangladesh

** Present address: East Nippon Expressway Company Limited (NEXCO EAST), Tokyo, Japan

Received 14 October, 2014

Accepted 27 January, 2015

©2014, Japan Society of Hydrology and Water Resources.

and the projected future air temperature from dynamical downscaling. We investigated $P_{99}(T)$ by analyzing 52 *in situ* stations in the Sapporo area compared with the CC rate of change. Future air temperatures projected by means of nine sets of dynamical downscaling using JMA's Non-Hydrostatic Model (NHM), Weather Research and Forecasting Model (WRF), and Regional Spectral Model (RSM) were performed over Hokkaido. Three different lateral boundaries for Max Planck Institute (MPI), Model for Interdisciplinary Research on Climate (MIROC), and National Center for Atmospheric Research (NCAR) GCMs were used to estimate $P_{99}(T)$ under climate change conditions. The next section introduces the methodology, and the results are shown in the following section. Finally, a summary is given.

METHODOLOGY

Data

The *in situ* data were obtained using the Sapporo Multi-sensors (SMS) network mainly operated by Sapporo City, which has 52 stations in Sapporo and its surrounding cities (Figure 1a). SMS provides precipitation intensity and air temperature data on a 10-min time scale from 1992 to 2011 (Kikuchi *et al.*, 2001; Sakazaki and Fujiwara 2008; Farukh and Yamada 2014). We analyzed the SMS dataset to investigate the relationship between $P_{99}(T)$ and the corresponding surface air temperatures. In fact, SMS provides precipitation and snowfall data individually and their measurement systems and measurement units also vary. So there is a small possibility of mixing up snowfall with precipitation in our analyses. The $P_{99}(T)$ was selected only for the hours during which we observed or simulated precipitation more than or equal to 0.5 mm h^{-1} against every 2°C , and the definition of $P_{99}(T)$ for observation and model output data is the same. The JMA measures several meteorological variables by radiosonde twice per day in Sapporo (9:00 and 21:00 LST). We estimated saturated water vapor amount ($SWV_{99}(T)$), precipitable water ($P_{99}(T)$) and the Showalter stability index ($SI_{99}(T)$) in the Sapporo area when $P_{99}(T)$ was observed. The radiosonde measurement is limited to only twice a day. Furthermore, the vertical temperature gradient above around the 700 hPa level was missing (which is evident from SkewT-LogP diagram and the raw data) for many of the radiosonde observations. Due to these reasons, $SWV_{99}(T)$ was calculated by vertically integrating the saturated water vapor from the surface to the tropopause assuming that the temperature decreases at the lapse rate of 0.65°C per 100 m from the prescribed surface temperature.

The relationship between $P_{99}(T)$ and air temperature in the Tokyo area (Figure 1b) was also investigated. In the Tokyo area, we analyzed a precipitation dataset measured by the Tokyo Metropolitan Government, where the availability and accuracy of *in situ* data are reliable from a strong data measurement network with good spatial coverage (e.g., Kusaka *et al.*, 2010). In this area, the total number of rain gauges is 69 and the measurements were performed from 1991 to 2004. To estimate $P_{99}(T)$ against air temperature, we used the nearest Automated Meteorological Data Acquisition System (AMeDAS) which is maintained by the JMA.

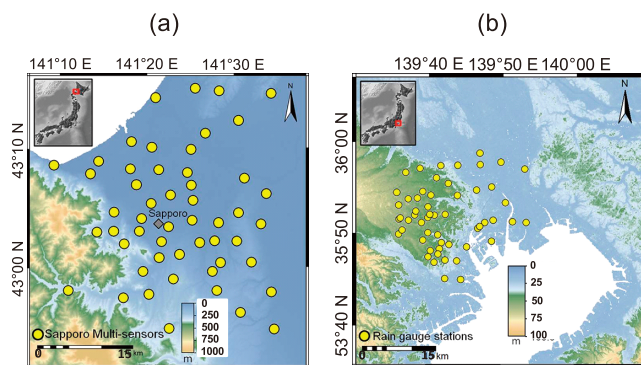


Figure 1. Geographic distribution of observational sites in the (a) Sapporo and (b) Tokyo areas. Yellow circles indicate locations of rain gauge stations

Dynamical downscaling

Giorgi and Bates (1989) explained dynamical downscaling as a modern technique to estimate the climate change effect in a particular domain through a RAM nested in lower-resolution boundary conditions derived from a GCM. In this study, a dynamical downscaling was performed over all of Hokkaido and its vicinity areas ($38\sim 50^\circ\text{N}$ and $135\sim 150^\circ\text{E}$) with an approximately 10-km spatial resolution using three RAMs referred to as NHM (Saito *et al.*, 2006), WRF (Skamarock *et al.*, 2008), and RSM (Juang and Kanamitsu, 1994; Kanamaru and Kanamitsu, 2007). All of these RAMs are widely used in dynamical downscaling or operational forecast experiments. The lateral boundary conditions used for the dynamical downscaling were from MPI (Roeckner *et al.*, 2003), MIROC (Hasumi and Emori, 2004), and NCAR (Collins *et al.*, 2006) GCMs both in the current i.e., 20th century experiment (20C3M) and future climate conditions on the Special Report on Emissions Scenarios (SRES) A1B (Meehl *et al.*, 2007). We conducted 10-year simulations for both current and future climates. For the future simulations, a 10-year period with a global 2°C air temperature increase was analyzed (MPI: 2060–2069; MIROC: 2050–2059; NCAR: 2080–2089) against a 10-year period between 1990 and 1999 for the current simulations. The simulated air temperature in the Sapporo area was used to investigate the future $P_{99}(T)$ after applying a correction to remove the model bias. Note that all the models showed a temperature increase in the future state.

A method for estimating the future 99th percentile precipitation intensity (hybrid-downscaling)

A hybrid-downscaling approach combining both dynamical and statistical downscaling is applied to estimate the future $P_{99}(T)$. In this study $P_{99}(T)$ was investigated in both the Sapporo and Tokyo areas. We obtained $P_{99}(T)$ for each daily mean air temperature range at every 2°C . The same procedure was performed for nine sets of dynamically downscaled precipitation using NHM, WRF, and RSM all combined with MPI, MIROC, and NCAR lateral boundaries in the 20C3M and A1B scenarios. The relationship between $P_{99}(T)$ and the air temperature was applied to the future projected air temperature after excluding the influence of model biases using the following steps: i) we investigated the 99th

percentile precipitation intensity and air temperature to obtain the regression function of the 99th percentile precipitation intensity as a function of air temperature; ii) we corrected the future projected air temperature for model bias by adding the difference between the simulated and observed air temperature for the current to the simulated future air temperature; iii) we applied the bias-corrected air temperature to the regression function for each SMS station; iv) the above three procedures were applied with different model results; and v) we estimated the future $P_{99}(T)$ using different sets of NHM, WRF, and RSM and three different GCM projections as the multi-model ensemble result.

RESULTS

Ninety-ninth percentile hourly precipitation intensity

Figure 2a shows $P_{99}(T)$ based on observation data in the Sapporo (blue circles) and Tokyo (red circles) areas. The dashed lines indicate the CC rate of change. Green asterisks show $SWV_{99}(T)$. In the Sapporo area, $P_{99}(T)$ follows the CC rate of change between 0°C and 23°C. A similar characteristic was also evident in the Tokyo area, where $P_{99}(T)$ follows the CC rate of change until around 26°C. Note that the rate of change is similar but not exactly the same. The tendency could be related to the lower number of precipitation events (only 90 events in a 25°C air temperature range during our

target period in the Sapporo area), in addition to the decrease in the wet-event duration (Utsumi *et al.*, 2011). The light blue squares in Figures 2a and 2c indicate $PW_{99}(T)$. In Figure 2c, error bars were calculated for every 5°C. As shown in Figure 2c, $PW_{99}(T)$ follows the CC-like rate of change along with the saturation vapor pressure for water (Figure 2b), as well as that of precipitation. The difference between $SWV_{99}(T)$ and $PW_{99}(T)$ is the amount between the maximum limit of water vapor and the actual water vapor when the 99th percentile precipitation intensity occurs. The difference between $PW_{99}(T)$ and $P_{99}(T)$ indicates the efficiency of precipitation against the actual amount of water vapor.

Figure 2d shows the $SI_{99}(T)$ against air temperature in the Sapporo area. $SI_{99}(T)$ decreases with an increase in air temperature, and the change is noticeably steep within the 10–20°C temperature range, similar to $P_{99}(T)$ and $PW_{99}(T)$. Therefore, the reason why $P_{99}(T)$ follows the CC-like rate of change can be explained by the characteristics of the amount of water vapor and vertical instability.

Future 99th percentile precipitation intensity

To avoid the limitation of sample numbers in warmer temperature ranges, $P_{99}(T)$ was averaged among 52 SMS stations within each air temperature range (Figure 3). In this panel, blue circles indicate the spatially averaged $P_{99}(T)$ expressed as $\bar{P}_{99}(T)$. Its standard deviation (SD) among 52

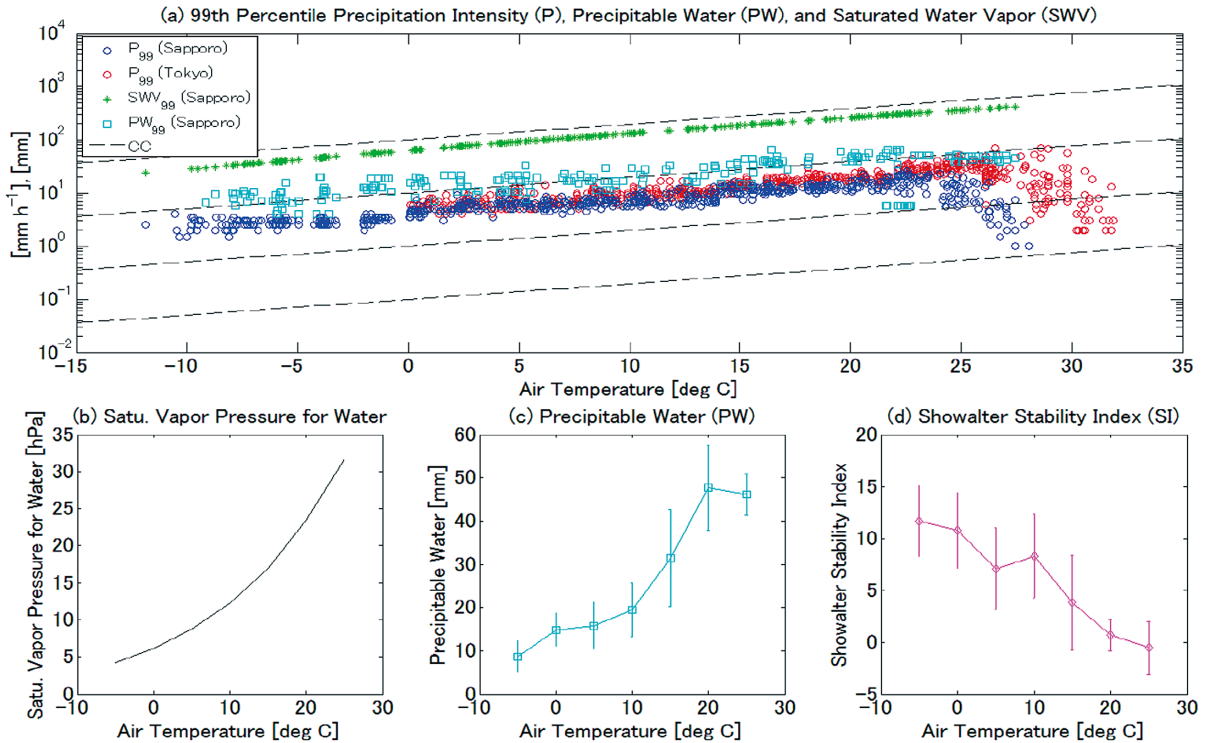


Figure 2. (a) Ninety-ninth percentile precipitation intensity [mm h^{-1}] against daily mean 2m height air temperature [$^{\circ}\text{C}$] in the Sapporo (blue circles) and Tokyo (red circles) areas. Precipitable water amount (light squares) [mm] and saturated water vapor (green asterisks) [mm] at 99th percentile precipitation intensity in the Sapporo area are plotted. The dashed lines indicate the CC rate of change. (b) Saturation vapor pressure for water [hPa]. (c) Same as precipitable water [mm] at 99th percentile precipitation intensity in the Sapporo area. (d) Showalter stability index at 99th percentile precipitation intensity in the Sapporo area. In (c) and (d), error bars indicate the standard deviations of each variable for each 5°C air temperature range

SMS stations is shown by blue whiskers. The blue solid line is the regression line of $\bar{P}_{99}(T)$ and is expressed as:

$$\bar{P}_{99}(T) = \frac{10^{0.02587T+1.99}}{24} \quad (1)$$

where, T is the air temperature ($^{\circ}\text{C}$). Here, we name Equation (1) as “equation of the 99th percentile hourly precipitation intensity in Sapporo.”

Figure 4 shows multi-GCMs with multi-RAMs ensemble mean $\bar{P}_{99}(T)$ for both current (blue circles; $\bar{P}_{99,MP}(T)$) and future (red circles; $\bar{P}_{99,MF}(T)$) climate conditions. The blue and red solid lines with shading denote the positive standard deviations (+SD) for current and future climate conditions, respectively (due to some negative values the $-SD$ is not shown here in a log scale). The subscripts MP and MF denote current (P) and future (F) climates in the model simulations. The blue thick line indicates the spatially averaged $P_{99}(T)$ which is expressed by Equation (1). In multi-GCMs with multi-RAMs ensemble mean, both the $\bar{P}_{99,MP}(T)$ and $\bar{P}_{99,MF}(T)$ behave almost similarly for positive temperature ranges up to approximately 24°C . But $\bar{P}_{99,MP}(T)$ dropped in the case of temperatures below -5°C . Although $\bar{P}_{99,MF}(T)$ showed an increasing trend up to 24°C , almost a similar trend between $\bar{P}_{99,MP}(T)$ and $\bar{P}_{99,MF}(T)$ can be seen up to about 22°C . Therefore, as the multi-model ensemble results suggest, such an increasing trend of air temperature range will be conserved in the future climate conditions.

Fujibe (2013) also revealed an increase of extreme short-term precipitation over Japan after 1980 in accordance with the rapid temperature increase. Lenderink *et al.* (2011) showed hourly extreme precipitation had a dependence of over $10\% \text{ K}^{-1}$ on air temperature. Nevertheless, based on the results of our study it could be assumed that Equation (1) can be applied to the future climate projections. Furthermore, according to Figure 2a $P_{99}(T)$ increases for temperatures of up to approximately 26°C in the Tokyo area. Likewise, an increasing trend in $P_{99}(T)$ was found for temperatures ranging up to approximately 23°C in the Sapporo area. This

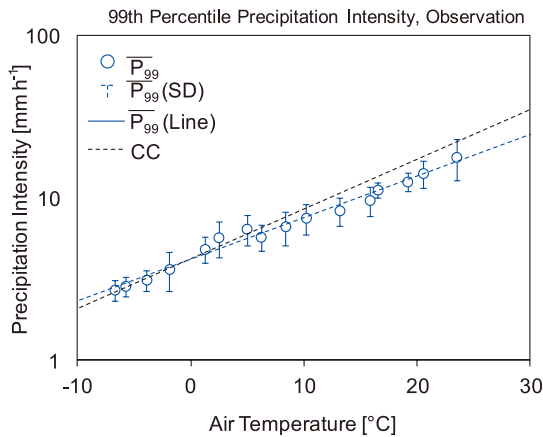


Figure 3. Relationship between spatially averaged 99th percentile precipitation intensity [mm h^{-1}] in the Sapporo area (blue circles) and its standard deviation at each air temperature (blue whiskers). The dashed lines indicate the CC rate of change

result could support our assumption that $P_{99}(T)$ in the Sapporo area will increase under future climate conditions. Several studies have found that climate models have difficulties in simulating $\bar{P}_{99}(T)$ parallel to the CC rate of change (e.g., Allen and William, 2002; Muller *et al.*, 2011). This is one of the reasons why simulating extreme short-term precipitation using climate models is challenging, and this motivated us to devise an alternative method to estimate the extreme short-term rainfall intensity in the future climate by using the observational evidence.

Finally, the future $P_{99}(T)$ in four seasons (March–April–May (MAM); June–July–August (JJA); September–October–November (SON); December–January–February (DJF)) was estimated using Equation (1) and the projected air temperatures after removing the model bias at each SMS station. Figure 5 shows the number of SMS stations for $P_{99}(T)$ for both current (blue bars; observation) and future (red bars; multi-GCMs and multi-RAMs ensemble mean) climate conditions with their fitted histograms (black solid lines). For the current climate condition, $P_{99}(T)$ was calculated directly from 52 stations of the SMS dataset during the 20 years between 1992 and 2011. On the other hand, the future $P_{99}(T)$ for MPI (2060–2069), MIROC (2050–2059), and NCAR (2080–2089) GCMs was estimated under the condition that the global mean air temperature will increase by 2°C , while the red bars also indicate the multi-GCMs with multi-RAMs ensemble mean.

In the current climate condition, $P_{99}(T)$ in the Sapporo area varies from 5.2 to 6.2 mm h^{-1} for MAM, with an average value of 5.7 mm h^{-1} (see Figure 5a). The extensive rainy months JJA shows the maximum spread of $P_{99}(T)$ between 11.5 and 13.6 mm h^{-1} , with $P_{99}(T)$ centered at 12.5 mm h^{-1} .

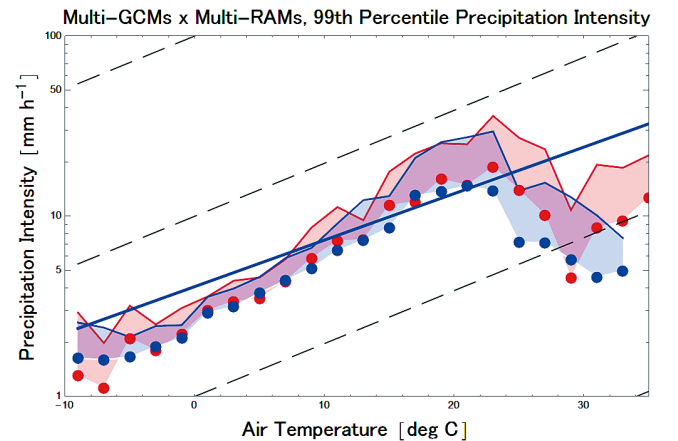


Figure 4. Multi-model ensemble mean 99th percentile precipitation intensity in the Sapporo area under the current (blue circles) and future (red circles) climate conditions dynamically simulated by NHM, WRF, and RSM with lateral boundary conditions from MPI, MIROC, and NCAR. The dashed lines indicate the CC rate of change, while the blue and red shadings represent positive standard deviations (+SD) for current and future climate conditions, respectively. Thick solid line indicates the spatially averaged 99th percentile precipitation intensity [mm h^{-1}] in the Sapporo area which is expressed as Equation (1)

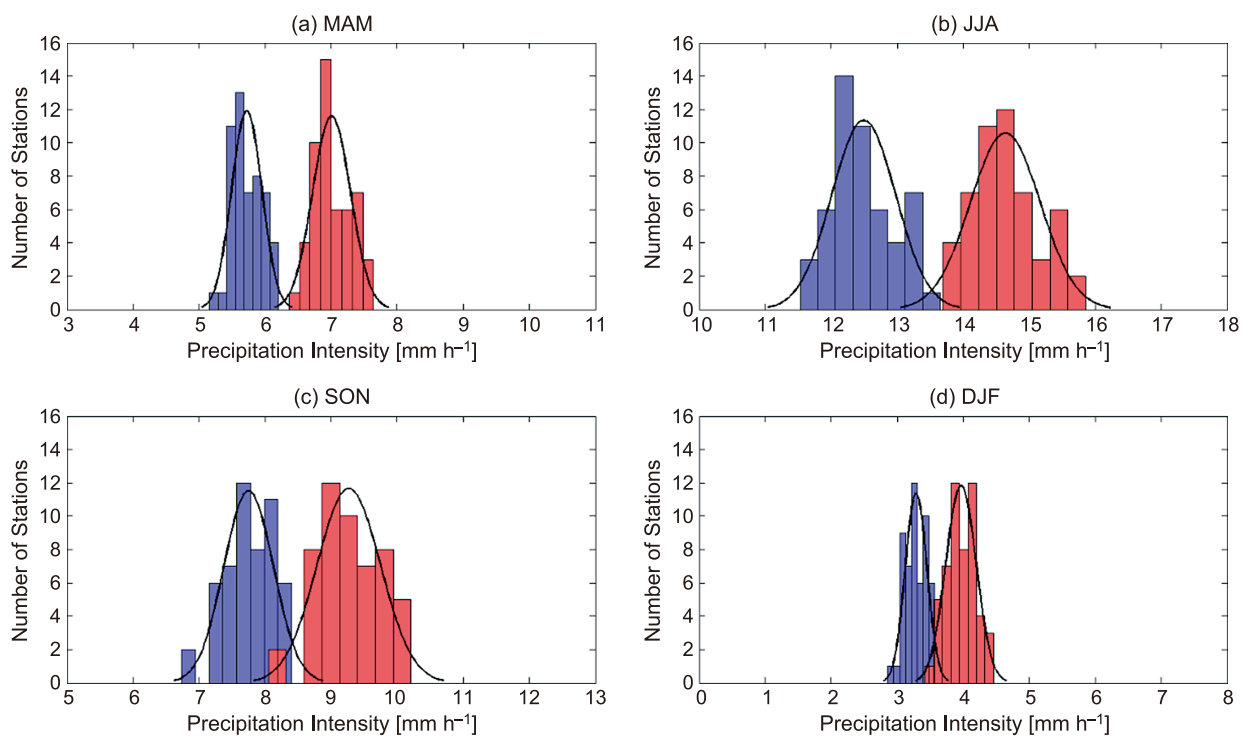


Figure 5. Relationship between observational and future projected 99th percentile precipitation intensity in four seasons. Blue bars indicate the observational 99th percentile precipitation intensity at 52 SMS stations and red bars for the future state as a multi-model ensemble result among multi-GCMs with multi-RAMs. The black curves show the normal distribution for all the individual cases

A moderate spread of $P_{99}(T)$ can be observed for SON (6.7 to 8.4 mm h⁻¹), whereas the minimum spread is found for DJF (2.9 to 3.6 mm h⁻¹). On the contrary, for the future climate state the ensemble mean shows $P_{99}(T)$ is centered at 7.0 mm h⁻¹ for MAM and varies between 6.4 and 7.6 mm h⁻¹ in the Sapporo area (Figure 5a). The maximum $P_{99}(T)$ spread (13.7 to 15.9 mm h⁻¹) would be in JJA while $P_{99}(T)$ is centered at 14.6 mm h⁻¹, and compared to current climate, a relatively lower number of stations would receive such a precipitation. Shifting of the center of the histograms along with significant $P_{99}(T)$ spreads are also evident for SON and DJF for the future climate state. The spread is more noticeable for SON from 8.1 to 10.2 mm h⁻¹, whereas in DJF a relatively larger number of stations will experience such precipitation. Therefore, combining all the seasons, the future $P_{99}(T)$ in the Sapporo area under the condition of a global 2°C temperature increase would trigger around a 1.2 fold increase of $P_{99}(T)$, whereas future projected air temperature would increase by 3.5°C for MAM, 2.8°C for JJA, 3.1°C for SON, and 3.3°C for DJF.

SUMMARY

This study investigated the 99th percentile hourly precipitation intensity against air temperature in the Sapporo and Tokyo areas. In both areas, the 99th percentile hourly precipitation intensity followed the CC-like rate of change (the dependence is not exactly the same but similar) until a threshold air temperature is reached. More specifically,

observation showed that the 99th percentile hourly precipitation intensity follows the CC-like rate of change until around 23°C and 26°C in Sapporo and Tokyo, respectively. We note that these findings should be interpreted cautiously because the results could have been affected by the limited number of precipitation events and a decrease in the wet-event duration. The precipitable water vapor and the convective instability (e.g., SI) followed the CC-like rate of change during the hours with the 99th percentile precipitation intensity. Dynamical downscaling using NHM, WRF, and RSM was performed over Hokkaido for both current and future climate conditions using different lateral boundary conditions for MPI, MIROC, and NCAR. The results showed that the gradient of the 99th percentile hourly precipitation intensity against daily air temperature among different climate conditions was similar in the Sapporo area. This result motivated us to show the observation based equation for the 99th percentile precipitation intensity in the Sapporo area that can be applied to a future state in which the global mean air temperature increases by approximately 2°C. Based on this assumption, we proposed a methodology named “hybrid-downscaling” to estimate the future 99th percentile precipitation intensity by combining the equation of the observation-based 99th percentile precipitation intensity and projected future air temperature using dynamical downscaling. This method can be applied to other areas in which a CC-like rate of change is found and the gradient of the 99th percentile precipitation intensity is conserved after dynamical downscaling under both current and future climate conditions.

ACKNOWLEDGEMENTS

The authors express their sincere gratitude to Professor Yasushi Fujiyoshi for his invaluable scholastic comments and suggestions, and encouragement to research on this issue. The authors also thank Sapporo City Office, Hokkaido and Tokyo Metropolitan Government, which provided an immense number of reliable datasets. Different datasets used for 99th percentile hourly precipitation intensity were obtained from various sources described in the second section. While the AMEDAS dataset can be downloaded freely from the JMA website (<http://www.jma.go.jp/jma/en/Activities/observations.html>), the other data should be obtained from the authors of the references provided in the paper. This study was partially supported by Research Program on Climate Change Adaptation (RECCA), MEXT, Japan, the MEXT SOUSEI program (theme C-i-C), the CREST/JST, and JSPS KAKENHI Grant Number 26242036.

REFERENCES

- Allen MR, William JI. 2002. Constraints on future changes in climate and the hydrologic cycle. *Nature* **419**: 224–232. DOI: 10.1038/nature01092.
- Collins WD, Bitz CM, Blackmon ML, Bonan GB, Bretherton CS, Carton JA, Chang P, Doney SC, Hack JJ, Henderson TB, Kiehl JT, Large WG, McKenna DS, Santer BD, Smith RD. 2006. The community climate system model version 3 (CCSM3). *Journal of Climate* **19**: 2122–2143. DOI: 10.1175/JCLI3761.1.
- Emergency and Disaster Information Service (EDIS). RSOE EDIS – Emergency and Disaster Information Service. <http://hisz.rsos.hu/alertmap/index2.php>. Last access January 21, 2015.
- Farukh MA, Yamada TJ. 2014. Synoptic climatology associated with extreme snowfall events in Sapporo city of northern Japan. *Atmospheric Science Letters* **15**: 259–265. DOI: 10.1002/asl2.497.
- Fujibe F. 2013. Clausius–Clapeyron-like relationship in multi-decadal changes of extreme short-term precipitation and temperature in Japan. *Atmospheric Science Letters* **14**: 127–132. DOI: 10.1002/asl2.428.
- Giorgi F, Bates GT. 1989. The climatological skill of a regional model over complex terrain. *Monthly Weather Review* **117**: 2325–2347. DOI: 10.1175/1520-0493(1989)117<2325:TCSOAR>2.0.CO;2.
- Hasumi H, Emori S. 2004. K-1 coupled GCM (MIROC) description. *K-1 Technical Report 1*, CCSR, University of Tokyo, Tokyo; 34.
- Intergovernmental Panel on Climate Change (IPCC). 2014. Working Group II, *IPCC 5th Assessment Report (AR5)*, Yokohama, Japan, 25–29 March 2014 – Changes to the underlying scientific/technical assessment to ensure consistency with the approved summary for policymakers (XXXVIII/Doc.4, Corr.2).
- Juang HM, Kanamitsu M. 1994. The NMC nested regional spectral model. *Monthly Weather Review* **122**: 3–26. DOI: 10.1175/1520-0493(1994)122<0003:TNNRSM>2.0.CO;2.
- Kanamaru H, Kanamitsu M. 2007. Scale-selective bias correction in a downscaling of global analysis using a regional model. *Monthly Weather Review* **135**: 334–350. DOI: 10.1175/MWR3294.1.
- Kharin VV, Francis WZ, Xuebin Z, Gabriele CH. 2007. Changes in temperature and precipitation extremes in the IPCC ensemble of global coupled model simulations. *Journal of Climate* **20**: 1419–1444. DOI: 10.1175/JCLI4066.1.
- Kikuchi K, Nagaishi Y, Asuma Y, Uyeda H, Kanemura N, Fujii M. 2001. Radar echo characteristics of the localized heavy snowfalls around Sapporo, Japan. *Journal of the Japanese Society of Snow and Ice* **63**: 239–251 (in Japanese).
- Kusaka H, Hanyu T, Nawata K, Furuhashi N, Yokoyama H. 2010. Examining local heavy rainfalls observed in Tokyo: case study of August 2 2002 and August 10 2004. *Journal of Heat Island Institute International* **5**: 1–10 (in Japanese).
- Lenderink G, Mok HY, Lee TC, van Oldenborgh GJ. 2011. Scaling and trends of hourly precipitation extremes in two different climate zones – Hong Kong and the Netherlands. *Hydrology and Earth System Sciences* **15**: 3033–3041. DOI: 10.5194/hess-15-3033-2011.
- Meehl GA, Collins WD, Friedlingstein PF, Gaye AT, Gregory JM, Kitoh A, Knutti R, Murphy JM, Noda A, Raper SCB, Watterson IG, Weaver AJ, Zhao ZC. 2007. Global climate projections. *Climate change 2007: The physical science basis*. Contribution of Working Group I to the Fourth Assessment Report of the Intergovernmental Panel on Climate Change. Solomon S, Qin D, Manning M, Chen Z, Marquis M, Averyt KB, Tignor M, Miller HL (eds.) Cambridge University Press: Cambridge; 747–845.
- Muller CJ, O’Gorman PA, Back LE. 2011. Intensification of precipitation extremes with warming in a cloud-resolving model. *Journal of Climate* **24**: 2784–2800. DOI: 10.1175/2011JCLI3876.1.
- Pall P, Allen MR, Stone DA. 2007. Testing the Clausius–Clapeyron constraint on changes in extreme precipitation under CO₂ warming. *Climate Dynamics* **28**: 351–363. DOI: 10.1007/s00382-006-0180-2.
- Peel MC, Finlayson BL, McMahon TA. 2007. Updated world map of the Köppen–Geiger climate classification. *Hydrology and Earth System Sciences* **11**: 1633–1644. DOI: 10.5194/hess-11-1633-2007.
- Roeckner E, Bäuml G, Bonaventura L, Brokopf R, Esch M, Giorgetta M, Hagemann S, Kirchner I, Kornbluh L, Manzini E, Rhodin A, Schlese U, Schulzweida U, Tompkins A. 2003. The atmospheric general circulation model ECHAM5. Part I: Model description. *Max Planck Institute for Meteorology Rep. 349*, 1–127.
- Saito K, Fujita T, Yamada Y, Ishida J, Kumagai Y, Aranami K, Ohmori S, Nagasawa R, Kumagai S, Muroi C, Kato T, Eito H, Yamazaki Y. 2006. The operational JMA nonhydrostatic mesoscale model. *Monthly Weather Review* **134**: 1266–1298. DOI: 10.1175/MWR3120.1.
- Sakazaki T, Fujiwara M. 2008. Diurnal variations in summertime surface wind upon Japanese plains: hodograph rotation and its dynamics. *Journal of the Meteorological Society of Japan* **86**: 787–803. DOI: 10.2151/jmsj.86.787.
- Skamarock WC, Joseph BK, Dudhia J, Gill DO, Barker DM, Duda MG, Huang X-Y, Wang W, Powers JG. 2008. A description of the Advanced Research WRF version 3. *NCAR Technical Note NCAR/TN-475+STR*, 113.
- Utsumi N, Seto S, Kanae S, Maeda EE, Oki T. 2011. Does higher surface temperature intensify extreme precipitation? *Geophysical Research Letters* **38**: L16708. DOI: 10.1029/2011GL048426.
- Yamada TJ, Sasaki J, Matsuoka N. 2012. Climatology of line-shaped rainbands over northern Japan in boreal summer between 1990 and 2010. *Atmospheric Science Letters* **13**: 133–138. DOI: 10.1002/asl.373.